We are IntechOpen, the world's leading publisher of Open Access books Built by scientists, for scientists

4,800
Open access books available

122,000
International authors and editors

135M
Downloads

Our authors are among the

154
Countries delivered to

TOP 1%
most cited scientists

12.2%
Contributors from top 500 universities

WEB OF SCIENCE™

Selection of our books indexed in the Book Citation Index in Web of Science™ Core Collection (BKCI)

Interested in publishing with us?
Contact book.department@intechopen.com

Numbers displayed above are based on latest data collected.
For more information visit www.intechopen.com

Chapter 2

Radiation Effects in Optical Materials and Photonic Devices

Dan Sporea and Adelina Sporea

Additional information is available at the end of the chapter

http://dx.doi.org/10.5772/62547

Abstract

The chapter continues previous reviews on radiation effects in optical fibers and on the use of optical fibers/optical fiber sensors in radiation monitoring, published by InTech in 2010 and 2012, by referring to radiation effects in optical materials, with an emphasis on those operating from visible to mid-IR, and on some photonic devices such as optical fibers for amplifiers, fiber Bragg gratings and long period gratings. The focus is on optical materials and fiber-based devices designed for both terrestrial and space-borne applications. For the presented subjects, an overview of available data on X-rays or gamma rays, electron beams, alpha particles, neutrons, and protons effects is provided. In addition, comments on dose rate, dose, and/or temperature effects on materials and devices degradation under irradiation are mentioned, where appropriate. The optical materials and photonic devices reliability under ionizing radiation exposure is discussed as well, as the opportunities to use them in developing radiation sensors or dosimeters. The chapter includes an extensive bibliography and references to last published results in the field. Novel proposed applications of photonic devices in charged particle beam diagnostics, quasi-distributed radiation field mapping and the evaluation of radiation effects in materials for mid-IR spectroscopy are briefly introduced to the reader.

Keywords: radiation effects, optical materials, optical fibers, fiber Bragg grating, long period grating

1. Introduction

The goal of this chapter is to continue previous reviews on radiation effects in optical fibers [1] and on the use of optical fibers and optical fiber sensors in radiation related measurements [2],

by referring to radiation effects in optical materials and some photonic devices. According to this vision, the chapter is organized to cover the interaction of ionizing radiation with some optical materials and optical fibers, followed by a reference to radiation effects on some photonic devices based on optical fibers. The discussion addresses radiation effects produced by both energetic photons and charged particles, as appropriate [3]. In this context, an overview of some recently published results in the field is included, with a focus on original authors' contributions.

The terrestrial radiation environments where optical and photonics components can be found include, but are not limited to, high energy physics experiments, nuclear power plants [3], fusion installations as the International Thermonuclear Experimental Reactor – ITER, or the Laser Mégajoule – LMJ [4–8], high power laser installations [9], nuclear waste repositories [10], high energy physics [11, 12], medical equipments for diagnostics or treatment [13]. On the other side, applications of optical components or photonic devices can be found in spaceborne instrumentation [14–16]. These environments involve various types of ionizing radiations, depending on the application considered: X-rays or gamma rays, electron beams, alpha particles, neutrons, protons, and Bremsstrahlung [3, 14, 17].

2. Radiation effects in optical materials

2.1. Optical materials

Extensive research was involved in the elucidation of defects formation in glasses, as investigations were performed in glasses with various compositions under ionizing and non-ionizing radiation exposure. The studies were focused either on the materials degradation upon irradiation or on the possible use of such materials in radiation dosimetry [18, 19]. The radiation induced changes depend on the glass composition, total dose, dose rate, temperature and humidity during exposure, and post irradiation heating of the sample [19]. The operation of a glass-based dosimeter can be decided as function of radiation sensitivity, linearity of the response, stability of the radiation produced effect, and possibility to re-use the material.

Besides glass-based optical materials, radiation hardening tests were performed on various other optical materials. More than 20 years ago radiation induced defects were studied in BaF_2 crystals by exposing them to gamma rays (from 10 Gy to 47 kGy) and observing the optical attenuation recovery (between 300 and 700 nm) under UV radiation and the scintillating signal [20]. Samples from different manufacturers exhibited radiation induced attenuation (RIA) saturation starting from 10^2 Gy. Crystal impurities and defects are the primary source of the optical attenuation increase in the 190–250 nm and 500–600 nm spectral bands induced by gamma rays [21]. BaF_2 and LaF_3 were subjected to Ne and U ions (at energies from 1.4 to 13.3 MeV/u) bombardment, and their degradation was investigated by scanning force microscopy (SFM), optical spectroscopy and surface profilometry. RIA for BaF_2 shown an increase at λ = 240, 420, 550 and 750 nm, while LiF_3 crystals remained almost unchanged spectrally. Surface topography studies indicated the presence of hillock in the irradiated zone [22].

Neutron irradiation was done on $Y_3Al_5O_{12}$, CaF_2 and LiF and RIA was monitored for UV-visible spectra. For $Y_3Al_5O_{12}$ samples an increase of the optical attenuation was present for wavelength

lower than 350–400 nm. CaF_2 and LiF single crystals degrade their optical transmission after neutron exposure mostly in the 400–500 nm region. When heated after the irradiation RIA for the three crystals recovers according to different patterns [23].

Gamma irradiation (dose rate 110 Gy/h, total doses of 500 Gy, 2 kGy, 8 kGy, 20 kGy) was conducted on CaF_2, Fused Silica and Clearceram in order to evaluate their qualification for space applications. RIA modification was measured over the 350–800 nm spectral interval at normal incidence. The optical investigations were completed by ellipsometry tests before and after the irradiation, from 200 nm to 1 μm. In the case of Clearceram, for example, three absorption bands located at 3.20, 2.20, and 1.81 eV are present. Over a quite long period these peaks decrease exponentially [24].

The scintillation properties of different optical materials were studied for their possible use in the development of radiation detectors. Two radiation induced luminescence (RIL) bands were observed in polycrystalline BaF_2 irradiated by X-rays at 295 K, for the wavelengths intervals 380–600 nm and around 659 nm [25]. Under X-ray irradiation, ZnSe crystals present a degradation of the optical transmission at 475–575 nm, and four luminescence spectra at λ = 460 nm, 610 nm, 645 nm and 970 nm [26]. An X-ray induced RIL peak was reported in CaF_2 crystals at λ = 420 nm, accompanied by a small one at about 350 nm [27].

Sapphire is one of the most intensively studied optical material under different ionizing radiation: X-ray (40 kV, 15 mA) and β from a ^{90}Sr source at 1.5 Gy/min [28]; 8 MeV proton (flux 2×10^{12} p cm^{-2} s^{-1} and 150 MeV argon (4.3×10^8 ion cm^{-2} s^{-1}) and 253 MeV krypton (4.3×10^8 ion cm^{-2} s^{-1}) [29]; gamma rays (dose rate 6.7 Gy/s, total dose 10^8 Gy) combined with neutrons (energy 2.4 MeV and fluences of 10^{17}–10^{20} n cm^{-2}) [30]; fast neutrons (energy 1.2 MeV and fluence of 1.4×10^{18} n cm^{-2}) [31], neutron irradiation followed by heating (energy 10 MeV, flux of 6.6×10^{12} n cm^{-2} s^{-1} and fluence up to 10^{19} n cm^{-2}), maximum temperature 1000°C) [32]. Sapphire proved to be radiation hardened under gamma exposure up to high doses (10^8 Gy), but is more susceptible to optical transmission degradation under gamma-neutron irradiation as the optical attenuation increases with the fluence for wavelengths below 600 nm. RIL spectra change under gamma irradiation in relation to RIA modification [30]. For fast neutron irradiation, absorption bands develop at λ = 203, 255, 300, 357 and 450 nm, while post irradiation excitation produce photoluminescence signals at λ = 320, 377 and 551 nm [31]. High purity Al_2O_3 crystals present absorption peaks at λ = 206, 230, 258, 305, 358 and 452 nm, when irradiated by fast neutrons. Post irradiation annealing (up to 1000°C heating) contributes to partial recover of RIA. Excitation at λ = 302 nm induces luminescence at λ = 325, 482, 543 nm [32]. The RIL associated to the F- and F^+- bands was found to be dependent on the proton dose [29].

The invention of quantum cascade laser (QCL) [33] and subsequent research in the field made possible the development of compact, very accurate, and portable spectroscopic instruments for the mid-IR spectral range of interest for organic compounds identification (3–12 μm). Tunable QCLs or arrays of QCLs operating at different wavelengths proved to be affordable substitutes for Fourier transform IR (FTIR) systems to be used in astronomy, astrophysics, astrochemistry, and space missions [34, 35]. In order to operate reliably under extreme conditions as components to be included in spaceborne equipment, the composing parts of

such equipment have to be tested under specific radiation exposure. Within this context, a program to evaluate for the Romanian Space Agency passive and active mid-IR components is under way. In this chapter, reference will be made to tests carried out on mid-IR windows materials (CaF_2, BaF_2, ZnSe, and sapphire—Al_2O_3). The subjects of these investigations are COTS (components-on-the-shelf) products, manufactured in Europe and China. The windows have 10–25 mm diameter and a thickness of 2–3 mm. Considering the complex space radiation environments which can be encountered during extra planetary missions, irradiation tests were run under various irradiation conditions: gamma rays (dose rate of 5.7 kGy/h +/–1.8%, four irradiation steps at total doses of 0.1 kGy; 1 kGy; 10 kGy; 20 kGy), alpha particles (doses from 1.46×10^6 kGy to 5.79×10^6 kGy, depending on the window material, at three beam currents of 100, 200 and 300 μC, beam diameter 3–4 mm), protons (at 10^{15} p cm^{-2}, 10^{16} p cm^{-2}, 10^{17} p cm^{-2} fluences), electron beam (dose rate of 4 kGy/min, total dose – several kGy). Gamma and electron beam irradiation were performed in air at room temperature, while proton and alpha particle irradiation were done in vacuum [36–38]. Prior and after each irradiation step the samples were measured in relation to their optical transmittance and reflectance over the spectral range from 250 nm to 18 μm. **Figure 1** illustrates the setup for spectral reflectance evaluation, which was carried out with the Gooch and Housego OL Series 750 Automated Spectroradiometric Measurement System and the accessories (tungsten lamp and IR glower, diffracting gratings, integrating spheres, reflectance standards, optical detectors - Si & Ge, PbS, InSb and HgCdTe) appropriate to each spectral interval over which the measurements were done. Optical transmittance of the irradiated samples was used to assess the color centers generation (RIA) in mid-IR optical materials under various irradiation conditions (type of radiation, dose, and dose rate). In the mean time, during alpha particle irradiation the RIL was monitored on-line in order to associate this signal with the presence of some dopants/impurities. The peak wavelengths of the detected radioluminescence are: λ = 285 nm (Caf_2), λ = 405 nm (BaF_2), λ = 465 nm (ZnSe), and λ = 700 nm (Al_2O_3). Significant decrease of the optical transmission was obtained for CaF_2 and BaF_2, below 1 μm, while a drop of the optical transmission over the investigated spectral range (0.3–16 μm) was noticed for all the materials except for sapphire, case when the transmission change was smaller as compared to other mid-IR materials. For the same purpose, RBS (Rutherford backscattering spectrometry) measurements were done on the investigated samples.

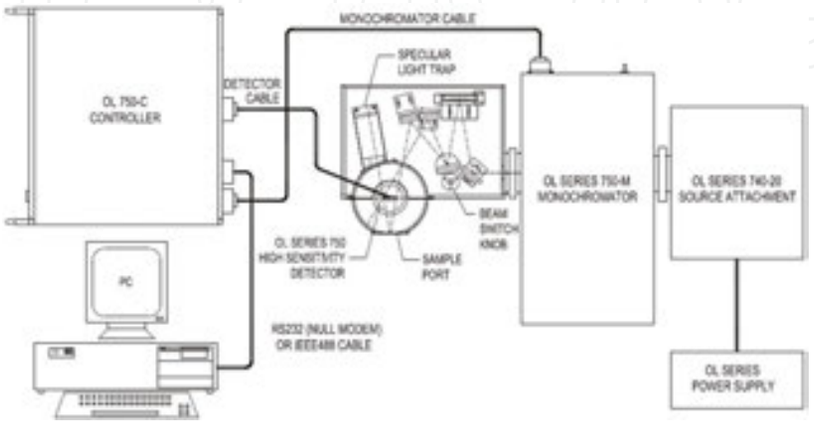

http://dx.doi.org/10.5772/62547

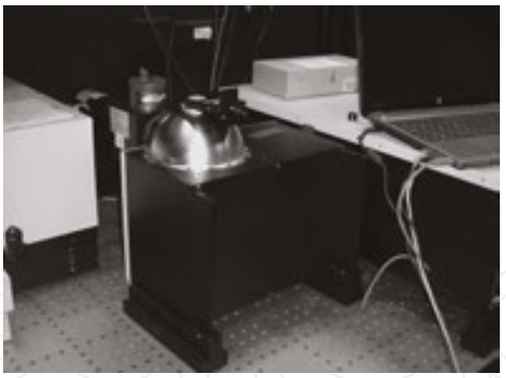

Figure 1. The sketch (a) and the picture (b) of the setup for spectral reflectance measurements over the UV to mid-IR (Reproduced with permission and courtesy of Gooch and Housego).

Spectral reflectance measurements were associated to optical microscopy tests as charged particles impinging on windows surface affect its quality (**Figure 2**).

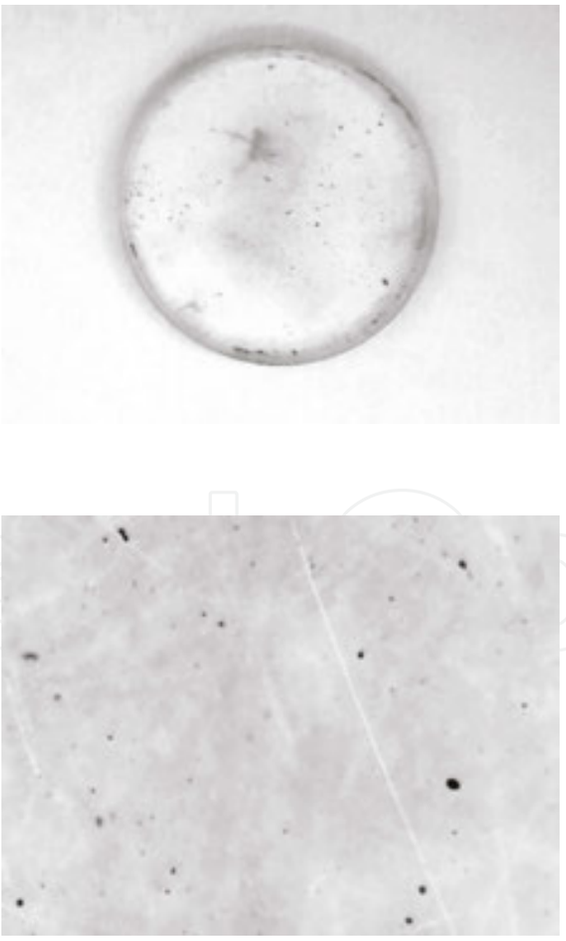

Figure 2. The degradation of windows surface quality after alpha particle irradiation: (a) BaF2; (b) ZnSe (Courtesy of Laura Mihai).

For the first time, THz (Terahertz) spectroscopy and imaging were introduced (**Figure 3**) in the analysis of irradiated mid-IR optical materials.

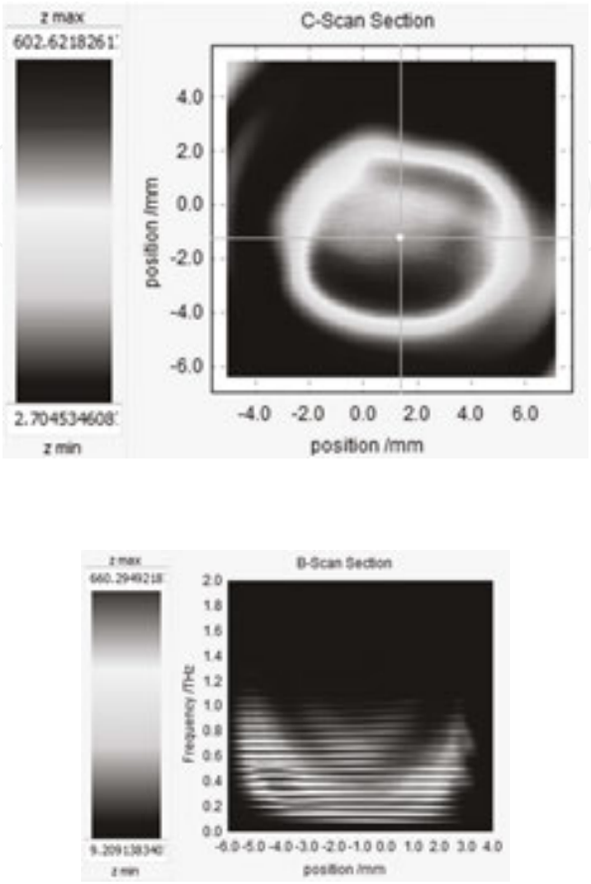

Figure 3. 2D plot of the THz reflected signal for BaF_2 window as the sample was scanned in the XY plane, for 0–2 THz (a); the frequency signal along the X axis (b), at a resolution of 50 μm (Courtesy of Laura Mihai).

2.2. Optical fibers

Optical fibers were suggested to be possible candidates for radiation dosimetry through RIA, RIL or thermoluminescence monitoring [2]. Such applications were considered in the case of glass optical fibers and plastic optical fibers as well. The radiation induced effects depends strongly on the optical fiber composition of the irradiated optical fibers, a detailed discussion on radiation induced defects in Pure Silica Core (PSC) and doped optical fibers can be found in [39, 40].

Optical fibers based on different dopants were proposed for radiation dosimetry using the optical attenuation change under gamma irradiation: TiO_2 and $GeO_2 + TiO_2$ in the silica core SM optical fibers [41]; Ge/Al co-doped SM fibers [42]; P_2O_5 doped step-index MM [43]. Depending on the experiment, low doses (dose rates of 0.01–1 Gy/h, for total doses up to 1 Gy) [43], moderate (dose rates 5–10 Gy/h, total doses of 10–100 Gy) [41] or high doses (dose rates of 2, 4 or 6 Gy/min, and the maximum total dose of 13 kGy) [42] were used. RIA was measured

either at λ = 980, 1310 and 1530 nm [41, 42] or at λ = 502, 540 and 560 nm [43]. The recovery of the irradiation induced attenuation was studied at room temperature, through photobleaching (Ar laser radiation at λ = 514 nm) or by heating the samples (1000°C in O_2 atmosphere at the pressure of 10 psi). Some of the studied samples (depending of the dopants concentration, wavelength considered, dose used, and radiation sensitivity) indicate a linear dependence of RIA with the dose, its independence with the dose rate and low recovery, which provide the ground for applications in radiation dosimetry.

Step index multimode, 16.0 mole% P_2O_5 co-doped (with and without 6.0 mole% GeO_2 in the core) optical fibers were tested under gamma irradiation and shown a linear response at 505 nm for dose rates of 0.1 to 1 Gy/h, and a radiation sensitivity of 0.69–0.97 dB m^{-1} Gy, up to a maximum dose 1 Gy [44]. As the samples present an independence of the radiation response on the dose rate and a low recovery they seem to be suitable for medical dosimetry.

An investigation of gamma rays on polarization maintaining (PM) optical fibers to be used in interferometric fiber optic gyroscope (IFOG) for spaceborne assembles was carried out on three types of fibers: (i) pure-silica-core, (ii) P-doped (1 mol%), and germanium Ge-doped (15 mol %), as they were exposed to total doses of 100 Gy and 1 kGy. RIA was monitored over the spectral range 1100–1700 nm, with a focus on 1310 and 1550 nm. All the three fibers are more sensitive to radiation at 1550 nm than at 1310 nm, and the most degradation as it concerns RIA was observed in the case of the P-doped optical fiber [45].

On-line evaluation of gamma radiation produced RIA was investigated in 40 cm long Co/Fe co-doped alumino-silicate optical fibers fabricated by modified chemical vapor deposition (MCVD), and exposed to dose rates of 6.7, 18.4, 37.0, and 78.3 Gy/min, for 30 min to total doses of 201, 551, 1110, and 2348 Gy [46]. The measurements were done at 1310 nm with a Yokogawa AQ6370C optical spectrum analyzer. Following the irradiation, the attenuation in the doped fiber increases 258 times as compared to a reference optical fiber (SMF-28^{TM}), and a small decay of the RIA signal was noticed after the irradiation ended. An almost linear relationship was present between RIA and the dose up to a total dose of 2.4 kGy at 78.3 Gy/min, which recommend this optical fiber for radiation dosimetry, as RIA dose rate independence was observed.

The performances of Ce-doped alumino-phospho-silicate optical fibers without Au (5.0 wt.% Al_2O_3, 0.15 wt.% P_2O_5, 0.3 wt.% CeO_2) and with Au co-doping (5.1 wt.% Al_2O_3, 0.15 wt.% P_2O_5, 0.27 wt.% CeO_2, and 0.2 wt.% Au_2O_3), produced by MCVD, were evaluated under electron beam irradiation at energy of ~6 MeV up to the total doses of 10^{12} e/cm^2, 5×10^{12} e/cm^2, 10^{13} e/cm^2, 5×10^{13} e/cm^2, 10^{14} e/cm^2, and 2.5×10^{15} e/cm^2. RIA was monitored between 400 nm and 1100 nm, and post irradiation photobleaching under He-Ne laser radiation laser (λ = 543 nm) and UV. The results of the study indicated that the Ce/Au-doped optical fibers are more suitable for fiber-based dosimetry [47].

In the last years, the research focused also on the X-ray irradiation (10 keV energy) effects on various optical fibers: PSC, Ge-doped, P-doped, Fluorine-doped/ co-doped, in some cases the irradiation being combined with sample heating to 300°C [48, 49].

The irradiation outcomes in changing the optical fiber characteristics were investigated by on-line RIA measurements, confocal micro-luminescence (CML) and electron paramagnetic

resonance (EPR), for total doses up to 3 MGy (dose rate of 50 Gy/s). RIA modifications in the UV-visible spectral range for Ge/F co-doped optical fibers produced under different conditions (draw speed and tension) were monitored with a mini optical fiber spectrometer (Ocean Optics HR4000) and deuterium-halogen DH2000 light source. Almost complete recovery of the irradiation induced attenuation was observed at room temperature for λ = 360 nm, corresponding to Ge(1) defects, at room temperature during the day following the exposure [49]. For various production conditions and different chemical composition the RIA vs. total irradiation dose graph indicates a linear dependency up to the dose of 300 kGy.

An interesting aspect in the research of optical fiber behaviour exposed to radiation is represented by the evaluation of radiation induced changes as heating is applied to the investigated sample. Different types of multimode UV optical fibers (deep UV enhanced, high OH step-index; solarization resistant, high OH step-index; UV enhanced extended spectral response, H_2-loaded, step-index) were tested under gamma irradiation. In some circumstances, the samples were heated to 573 K while irradiated, as the variation of the optical attenuation at specific wavelengths in the UV spectral range (λ = 248 nm, λ = 265 nm, λ = 320 nm and λ = 330 nm) was monitored. For some wavelengths (λ = 248 nm and λ = 265 nm) H_2-loading improves radiation resistance, while heating during the irradiation of the same optical fiber increases their radiation sensitivity [50].

A complex research was carried out to evaluate the combined effect of radiation (1keV X-ray, 50 Gy/s dose rate and total dose from 1.5 KGy to 1 MGy) and heating up to 300°C, for different types of optical fibers [48]. The results of this investigation indicated that no unitary behavior with temperature during radiation exposure can be predicted in the case of PSC, Ge-doped, P-doped, Fluorine-doped optical fibers, as in some situations (fiber compositing, temperature range, total dose) the sample heating has no effect in compensating the defects generation, while in some others RIA increases or decreases with the temperature increase. In any case, some of the study conclusions refer (i) to the possible use of such fibers in radiation dosimetry, especially at low doses, and (ii) to the limited length of fiber which can be incorporated into distributed radiation sensing systems.

A recent contribution to the use of optical fibers in radiation dosimetry refers to some studies carried out in cooperation with a team working at the European Synchrotron Radiation Facility, in Grenoble on UV multimode optical fibers subjected to synchrotron radiation [51]. In this experiment were tested five types of commercially available UV optical fibers and off-line measurements concerning the degradation of the optical fibers transmission in the UV-visible spectral range were done, as color centers developed upon exposure to synchrotron radiation. The measurements were performed for different doses: 5, 10, 30, 60, 200, 400, 1000 and 2000 Gy. The radiation induced optical attenuation was monitored in relation to recovery phenomenon both at room temperature and after samples heating to 560 K. The change of optical transmission and the increase of the attenuation at specific wavelengths (λ = 215 nm; λ = 229 nm; λ = 248 nm; λ = 265 nm; λ = 330 nm) were performed using the setup presented in **Figure 4**. The measurements were done with a dedicated software control developed under LabVIEW, by using a broadband UV-visible light source, a sensitive optical fiber spectrometer, and an optical fiber multiplexer.

http://dx.doi.org/10.5772/62547

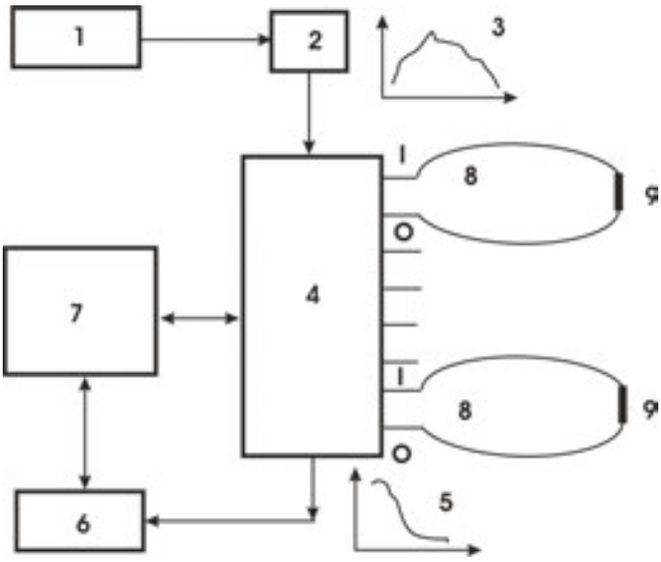

Figure 4. The sketch of the measuring setup: (1) light source; (2) optical fiber attenuator; (3) spectrum of the light source; (4) optical fiber multiplexer; (5) optical fiber sample absorption spectrum; (6) optical fiber mini spectrometer; (7) laptop; (8) connecting optical fibers; (9) irradiated optical fiber samples. I, multiplexer input; O, multiplexer output.

The graphical user's interface is illustrated in **Figure 5**. The multiplexer is employed to connect different tested samples to the light source and the spectrometer and help for the determination of the optical absorption from 215 nm to 600 nm. The operator can preset the number of averaging cycles, the box car value and can select the wavelengths of interest to be monitored. Of interest for these tests was to monitor specific wavelength associated to the presence of color centers in glass fibers. By observing the dependency of the optical absorption on the total irradiation dose at the specified wavelengths (**Figure 6**) can be estimated the linearity of this dependency and the spectral interval over which a saturation effect occurs. This can help to evaluate the possible use of these optical fibers in radiation dosimetry, at specified dose rates.

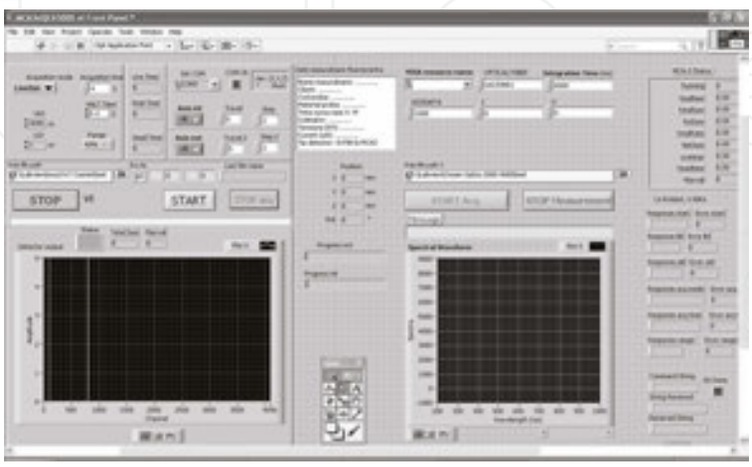

Figure 5. The LabVIEW graphical user's interface for the experimental setup (Courtesy of Laura Mihai).

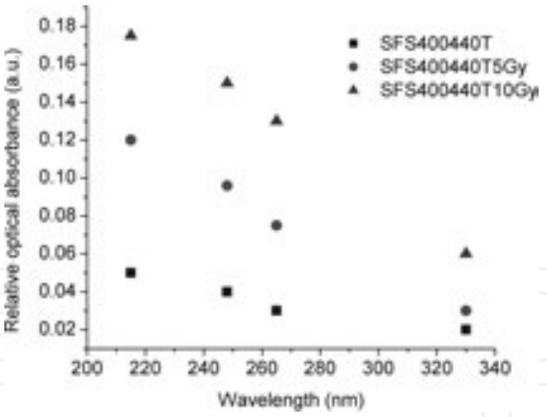
Relative optical absorbance (a.u.)
Wavelength (nm)
SFS400440T
SFS400440T5Gy
SFS400440T10Gy

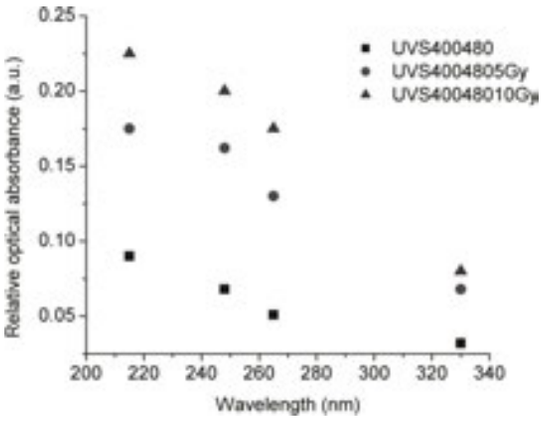
Relative optical absorbance (a.u.)
Wavelength (nm)
UVS400480
UVS4004805Gy
UVS40048010Gy

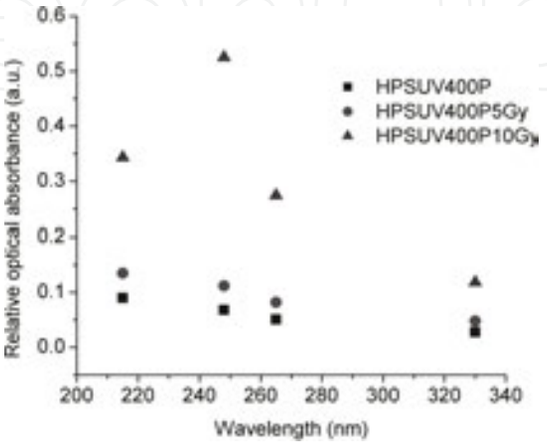
Relative optical absorbance (a.u.)
Wavelength (nm)
HPSUV400P
HPSUV400P5Gy
HPSUV400P10Gy

http://dx.doi.org/10.5772/62547

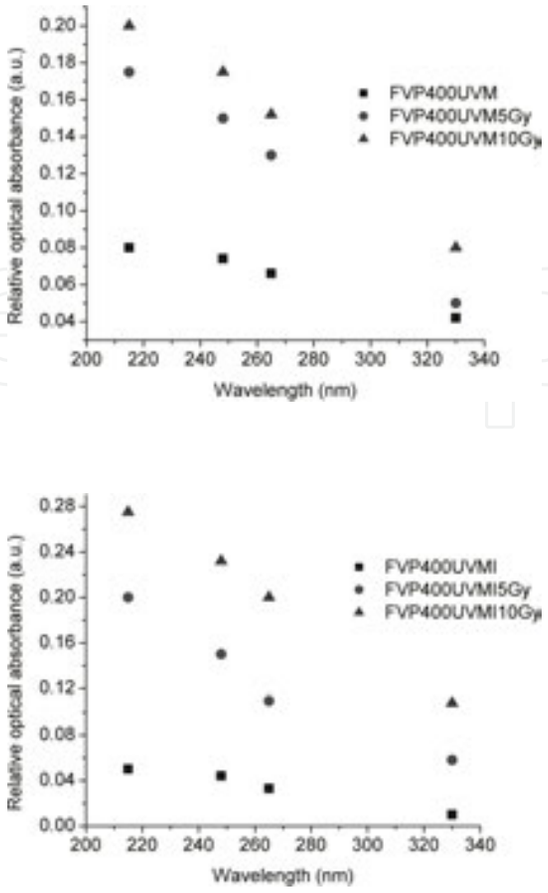

Figure 6. The dynamics of the color center formation as function of the dose (i.e. 5 Gy and 2000 Gy in this case) for the five tested optical fibers, at λ = 215 nm, λ = 248 nm, λ = 265 nm, λ = 330 nm: (a) SFS400/440T (Fiberguide Industries Inc.); (b) UVS400/480 (Fiberguide Industries Inc.); (c) HPSUV400P (Oxford Electronics); (d) FVP400/UVM (Polymicro Technologies); (e) FVP400/UVMI (Polymicro Technologies).

As a premiere, the use of THz spectroscopy and imaging to assess the synchrotron radiation induced changes in the core and coating of the investigated optical fibers (**Figure 7**) was reported. This approach makes possible the "visualization" of the dielectric constants change of the irradiated materials.

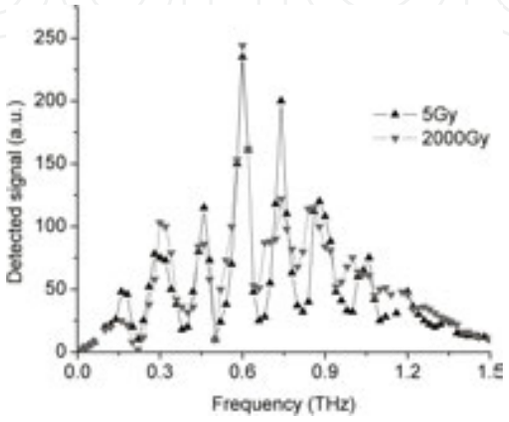

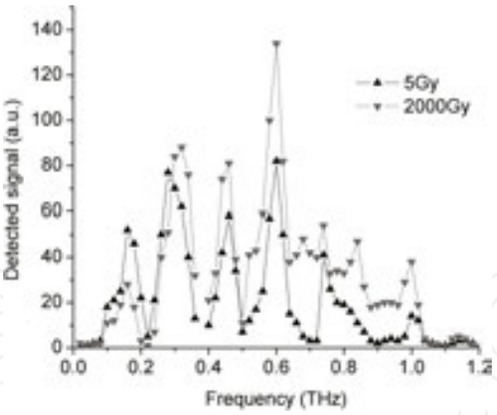

Figure 7. The THz spectral signal of the core (a) and coating (b) of an irradiated UV optical fiber, for two synchrotron radiation doses: 5 Gy and 2000 Gy (Courtesy of Laura Mihai).

The potential to employ P-doped core multimode optical fibers as X-ray (1 keV) radiation detectors for doses up to 3 kGy, under different dose rates (1, 10, 50 Gy/s) was studied by monitoring in real time the RIA in the spectral range from 200 to 900 nm. The results indicated a sub linear dependence of the irradiation induced attenuation with the dose and dose rate. The temperature did not change RIA during the irradiation for values between 5 and 50°C. The highest radiation sensitivity was observed at 300 nm, ~0.60 dB/m^{-1} Gy^{-1} [52].

For the case RIA values during the irradiation is dependent on the radiation dose and exhibit a recovery after the exposure is interrupted, a differential scheme can be applied when the measurand is represented by the difference of RIA at two wavelengths, $\lambda = 413$ nm and $\lambda = 470$ nm, respectively [53].

Another novelty recently introduced refers to the test of gamma radiation on perfluorinated polymer optical fibers (pPOF). These results complement the investigations previously reported in literature on the spectral characteristics of gamma irradiated PMMA optical fibers. In this case, commercially available MM perfluorinated fiber GigaPOF-50SR from Chromis Fiberoptics were exposed to gamma ray at a dose rate of 5.7 kGy/h for total doses of 1, 5, 20, 50 and 100 kGy. The irradiation took place at maximum temperature of 32°C, and the samples were measured before and after the irradiation using a ν-OTDR from Luciol Instruments, operating at 1310 and 1550 nm [54]. In addition, strain tests were also performed to evaluate the mechanical degradation of the polymer fiber under gamma irradiation. For doses up to 5 kGy the attenuation vs. the dose presents a linear dependency with a radiation sensitivity of 0.096 ± 0.006 dB m-1 kGy^{-1} at 1310 nm, and 0.25 ± 0.05 dB m-1 kGy^{-1} at 1550 nm. The obtained results suggest the possible use of these optical fibers in radiation dosimetry. The dynamics of the color centers formation under gamma irradiation was investigated by on-line measurements and by monitoring RIA change at several wavelengths ($\lambda = 420$, 525, and 750 nm). The highest radiation sensitivity was noticed at $\lambda = 420$ nm (up to 0.5 kGy) dose, while the best linearity response of RIA vs. dose was obtained at $\lambda = 750$ nm for a dose reaching 2.5 kGy [55].

The last decade recorded as a breakthrough the use of sapphire optical fibers in radiation environments, as sapphire supports very high operating temperatures and presents minor

optical transmission changes when exposed to ionizing radiation over a wide spectral range [56]. Recently, sapphire optical fibers were subjected to neutron flux of 1.5×10^{12} n cm^{-2} s^{-1} and a gamma dose rate of 84 kGy/hr (dose in sapphire) for a total neutron fluence of 1.1×10^{17} n cm^{-2} and total gamma dose of 1.8 MGy [57]. The optical attenuation in the sapphire fiber was measured on-line over the 500–2200 nm spectral range. The major RIA occurs below the 500 nm measuring limit. A change of RIA was noticed as the sample was heated to 1000°C, under gamma irradiation [58].

The use of optical fibers for distributed measurements in ionizing radiation environments became a hot topic in the last years as several tests were run and some possible applications were suggested: Raman and Brillouin strain/ temperature sensing [10, 59]; Rayleigh temperature sensing [60]. Tests were performed on standard communication, highly doped GeO_2, F-doped optical fibers [10, 59] and (PSC), Ge-doped, radiation hardened and Al-doped optical fibers [60], at dose rates of 700 Gy/h [60], 1.5 kGy/h [10], 28 kGy/h [59], and total doses of 110 kGy [60], 618 kGy [10], 10 MGy [59]. RIA proved to be the major challenge in using optical fibers distributed Brillouin temperature sensors, as the operating distance is reduced to several hundreds of meters due to irradiation [59]. Limitations in temperature monitoring are present also in the case of Rayleigh-based setup [60]. Temperature measurements using Raman scattering encounters some difficulties as the temperature evaluation uncertainty is quite high upon irradiation [10].

The complementary aspect of interest is represented by the possible use of radiation sensitive optical fibers for distributed dosimetry. Two approaches were proposed to be used: (i) the optical time domain reflectometry – OTDR [61], (ii) the optical frequency domain reflectometery – OFDR [62]. In both experiments the fiber samples were subjected to gamma irradiation: P-doped optical fibers [61] and standard communication, Al-doped, and P-doped optical fibers [62], at dose rates 590 Gy/h at 30°C and 605 Gy/h at 80°C, total dose of about 71 kGy [62], and dose rate of 23 mGy/s, for a total dose of 300 Gy [61]. The OTDR approach exhibits a limited spatial resolution for distributed dosimetry. Depending on the optical fiber type, the interrogating instrument dynamic range and the dose, the usable length of the dosimetric fiber is limited to several centimeters [62].

2.3. Rare earth-doped optical fibers

Generally, radiation hardening tests of rare earth-doped optical fibers were performed in relation to their possible use in space applications such as inter-satellite communications and fiber optic gyroscopes (FOGs) applications [63–65]. The investigations focused on the radiation induced absorption in the optical fiber and on changes of the emission efficiency. Tests were carried out under gamma ray [63, 65, 66], neutrons [65], protons [65–67], or X-ray [66] exposure. The reported studies indicate that:

- the irradiation results are primarily dependent on the dose and not on the type of irradiation involved [65],
- the device degradation is function more on the co-dopant concentration than on the rare-earth elements [65],

- annealing and photobleaching can contribute to partial recovery of the irradiation induced effects [65, 67, 68].

Tests on photobleaching of two Erbium-doped fibers (EDFs) subjected to 1.3 and 2.24 kGy gamma irradiation were carried out at two laser wavelengths (532 and 976 nm). A higher efficiency was achieved with the shorter wavelength excitation. The annealing effect induced by the 976 nm laser is comparable to that present in the case of thermal annealing at 500 K [69].

In another experiment, an EDF was tested under electron irradiation (beam energy 1.2 MeV, total dose 10 kGy), and the output power, noise figure and the central wavelength were measured after the irradiation, with the pump at 980 nm and detection at 1550 nm. The central wavelength did not change after irradiation, while the output power and noise figure were deteriorated (i.e. the output power dropped from 10 to –60 dBm for the same pump level). Within 2 weeks, the two parameters partially recovered [70].

Single mode and multi-mode Yb-doped optical fibers, acting as amplifiers at 1064 nm, were subjected to gamma rays and mixed gamma-neutron irradiation, up to a total dose of 1 Gy(Si) [71]. It was noticed a linear decrease of the output power with the irradiation dose. A slight recovery was observed at room temperature, after 20 hours.

In his PhD thesis, Fox [72] concluded that EDFs are more radiation sensitive than Yb^{3+}-doped fibers, and the most radiation hardened to gamma ray are optical fibers of Er^{3+}/Yb^{3+} co-doped type. In this investigation, the radiation induced degradation increases with the increase of the dose rate.

Optical fiber preforms of Yb-free aluminosilicate core, Yb-doped Al-free silicate core, Yb-doped alumino-silicate cores and Yb-free germanosilicate core produced by MCVD and solution-doping techniques were irradiated by 45 kV X-rays, at ~2.5 Gy(SiO_2)/ min, for doses up to 0.3–0.5 kGy [73]. The effects of the irradiation were studied by thermally stimulated luminescence (TSL) and optical absorption measurements.

Investigations were carried out to evaluate the influence of H_2-loading of EDFs, under pumping at 980 and 1480 nm, as the samples were subjected to gamma irradiation, having doses from 0.1 to 10 kGy. One such sample was a H_2-loaded EDF, while the other was H_2-free carbon-coated [74]. At 980 nm pumping a photobleaching effect was observed which increases the efficiency of the process especially in the H_2-loaded optical fiber. No such effect was present with the pump radiation of 1480 nm. H_2-loading and the use of a hermetical coating of the optical fiber, which prevents H_2 diffusion, produce a radiation resistant EDF [75].

One approach to enhance the radiation resistance of the optical amplifier consists in the use of Er-doped-nanoparticles optical fibers [76]. Another proposed method is based on the doping of the optical fiber core with Ce, reducing in this way the radiation sensitivity [77].

Tests on a thulium doped optical fiber amplifier were performed under neutron irradiation and a 17.1 dB was observed for a dose of 720 Gy, which is close to the computed values [78].

The development of Bi co-doped silica optical fibers [79] having an extensive emission operation range (from 1100 to 1800 nm) called researchers attention on their investigation

under ionizing radiation. Tests run under gamma irradiation, dose rate – 5.5 kGy/h and maximum total dose – 50 kGy, on Bismuth/Erbium/Ytterbium co-Doped Fiber – BEYDF ([Bi] ~ 0.07, [Er] < 0.1, [Al] ~ 0.35, [Ge] ~ 1.18, [Yb] ~0.02 atom%, respectively, indicated the formation of bismuth related active center (BAC), as the absorption at 830nm is increased significantly, while the absorption at longer wavelength diminishes [80].

In the case of Bi/Al-co-doped silica optical fibers the fluorescence peak increases with the increase of the gamma dose (dose rate, 800 Gy/h; maximum total dose, 3 kGy), when the sample is pumped at 980 nm. The preform of the investigated materials had the following concentrations: Si—28 mol/% (core), Ge— 6 mol/% (core), O—66 mol/% (core and inner layer), Bi—0.016 mol/% (core and inner layer), and Al—0.04 mol/% (core and inner layer). It is presumed that this enhancement of the photoluminescence signal upon irradiation is due to creation of subvalence Bi ions [81].

Another investigation was focused on the effect of gamma irradiation (dose rate – 5.5 kGY/h, total doses of 1, 5, 15, 30 and 50 kGy) on samples of Bismuth/Erbium co-doped fiber (BEDF). The irradiation has significantly increased unsaturable absorption by about 8 dB. This corresponds to a very significant unsaturable attenuation coefficient change of ~32 dB/cm. The results indicate that the saturable absorption of the BEDF at 830 nm is also increased by about 4 dB. This corresponds to a significant saturable attenuation coefficient change of 16 dB/cm. The increase in saturable pump absorption implies that the irradiation has significantly increased the number of bismuth related active centers (BAC-Si). In this case the overall emission at 1430 nm (which is related to BAC-Si) is only slightly decreased while the unsaturable absorption is significantly increased. A good radiation survivability of the BEDF for emission or amplification was noticed [82].

3. Radiation effects in photonic devices

3.1. Fiber Bragg gratings

Fiber Bragg gratings were excessively studied under various type of ionizing radiation: gamma ray [12, 83, 84], neutron [85], mixed gamma-neutron [86–88] or 13.5 MeV protons [89]. In most cases, the changes of the FBG Bragg wavelength are relatively low. Tests were carried out using Type I, Type II, Type IA, Type IIA, chemical composition or fs laser engraved gratings, and were focused on the effect of fiber composition, dose rate, total dose, heating during the irradiation or possible photobleaching during the exposure to ionizing radiation [90]. For example, Type I gratings produced in H_2-loaded standard communication optical fibers (SMF28™) or B/Ge co-doped optical fibers present an increase of the central wavelength followed by a plateau, with an overall change between 10 pm to 34 pm, under 0.54 MGy exposure. In the case of Type II gratings written in B/Ge co-doped optical fibers exhibit a decrease of the central wavelength between -30 and -60 pm. Degradation (30–50%) of gratings reflectivity was produced after irradiation, while no recovery was observed in the studied sensors [91]. A quite significant impact of gamma radiation on Ge-doped core optical fibers was observed as such uncoated fibers are immersed in water during gamma exposure [83], for

a total dose of up to 5 MGy. Generally, all the investigations carried out on radiation effects on FBGs focused on the possible use of such devices in radiation environments for temperature or humidity [12] monitoring. Under some design circumstances (optical fiber type, technology used to write the grating), these modifications are significant, making possible the use of FBGs as radiation detectors [92, 93].

More recently, the use of FBGs developed in sapphire optical fiber was proposed for monitoring very high temperature in nuclear reactors [94].

Through these studies, the paradigm was changed as [95]:

- FBGs were produced in radiation hardened optical fibers by two-beam interferometer and deep ultraviolet fs laser radiation;
- for the first time FBGs written in both standard commercial optical fibers and radiation hardener optical fibers were tested, exposed to the electron beam from a linear accelerator;
- a mash of FBGs was used for beam diagnostics of charged particle beams, as a novelty.

This research indicated a linear dependence of the Bragg wavelength shift with the irradiation dose for commercially available FBGs and grating produced in radiation hardened optical fibers, and this shift was monitored by measuring simultaneously with a thermocouple the temperature change in the irradiation plane. This aspect is important because no saturation or permanent modification of FBG wavelength was observed; hence these sensors can be used for on-line measurements. The principle of the charged particle beam diagnostics is illustrated in **Figure 8**, for the case of an electron beam having a diameter of about 100 mm. The spatial resolution is limited by the number of FBGs engraved in an optical fiber, their individual length and the distance between two adjacent FBGs. In the described proof-of-concept design, gratings having 12 mm and 4 mm length were employed. As compared to other solutions for charge particle beam monitoring (arrays of Faraday cups; ionization chambers; micro strip metal detector; pepper-pot device, slit-grid or rotating slits; scintillating screen or gas detector; flat panel detectors, arrays of p-i-n diodes; moving wire or vibrating wire scanners) there are several advantage of this approach: its immunity to electro-magnetic noise, remote monitoring capability and the possibility to multiplex the acquired signals by using few connecting lines.

The operation of the proposed instrument is similar to that employed for laser beam diagnostics. In the evaluation of a laser beam quality an image sensor is used to acquire the transversal distribution of the laser beam's intensity. Periodically, the electric charge generated inside the image sensors is removed upon reading and new acquisition starts. In this implementation the instrument operation is based on the proved reliability of the tested FBGs under electron beam exposure and on the linear shift of FBGs Bragg wavelength with the temperature in the detection plan, and hence with the deposed energy by the charge particle beam. Prior to the use, the FBGs were calibrated as it concerns their wavelength change vs. temperature.

When the charge particle beam (1) is propagating from the linear accelerator output (2) its diameter increases (4) in the detection plan (5) due to its divergence (**Figure 8a**). In the detecting plan (item 1 in **Figure 8b**) a mesh composed of FBGs (3) is placed, the sensors being embedded into a thermally insulating material to prevent the lateral dissipation of the heat. As the

http://dx.doi.org/10.5772/62547

individual gratings are exposed to different beam energies their temperature increases according to the energy deposed on each detecting site. In this way, in time, a map of the transferred energy at each location is obtained.

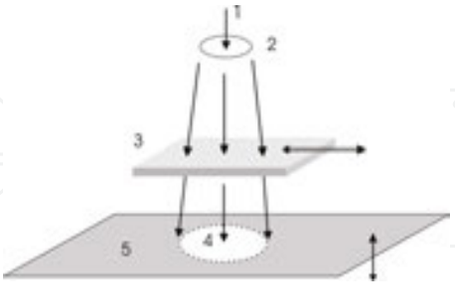

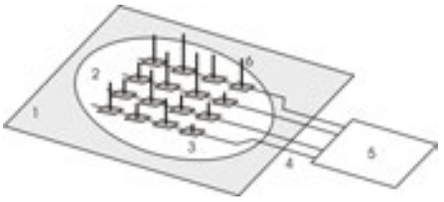

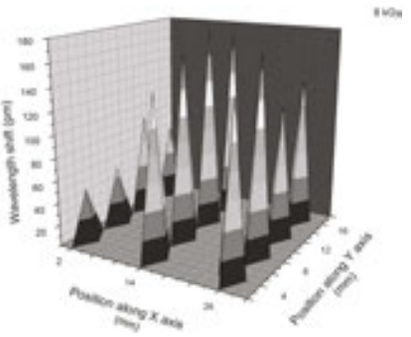

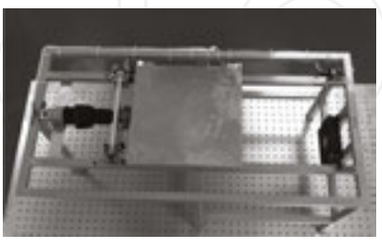

Figure 8. The operation principle of the electron beam analyzer: (a) the moving shutter used to interrupt FBGs exposure to the electron beam: (1) the incident electron beam; (2) beam diameter at the exit of the linear accelerator focusing system; (3) moving shutter; (4) the electron beam diameter at its incidence on the detection plan; (5) detecting plan. (b) The position of the FBGs mash: (1) the detecting plan; (2) electron beam pattern on the detection plan; (3) FBGs; (4) connecting optical fibers; (5) optical fiber interrogator; (6) bars symbolizing the integral energy deposited on a particular FBG at a specified moment. (c) Example of the data acquired for the 8 kGy dose [95]. (d) Top view of the shutter and cooling system.

The detector operates as an energy integrator (dose related measurements). Permanently, the central wavelength of all sensors is acquired by a Micron Optics optical fiber interrogator, which makes possible the real time mapping of the electron beam cross section energy distribution. In order to avoid saturation, periodically the FBGs signal has to be "reset" by blocking the electron beam and forced cooling the FBGs array. For this purpose a thick (20 mm) Al shutter restricts under the software control (**Figure 8a** and **8d**) the exposure of the FBGs by interrupting the electron beam. During the interval the beam is blocked, a cooler pushes air over the sensors' matrix. The Al shutter goes back and forth as the array has to be exposed or cooled. The flow chart for the instrument operation is presented in **Figure 9**.

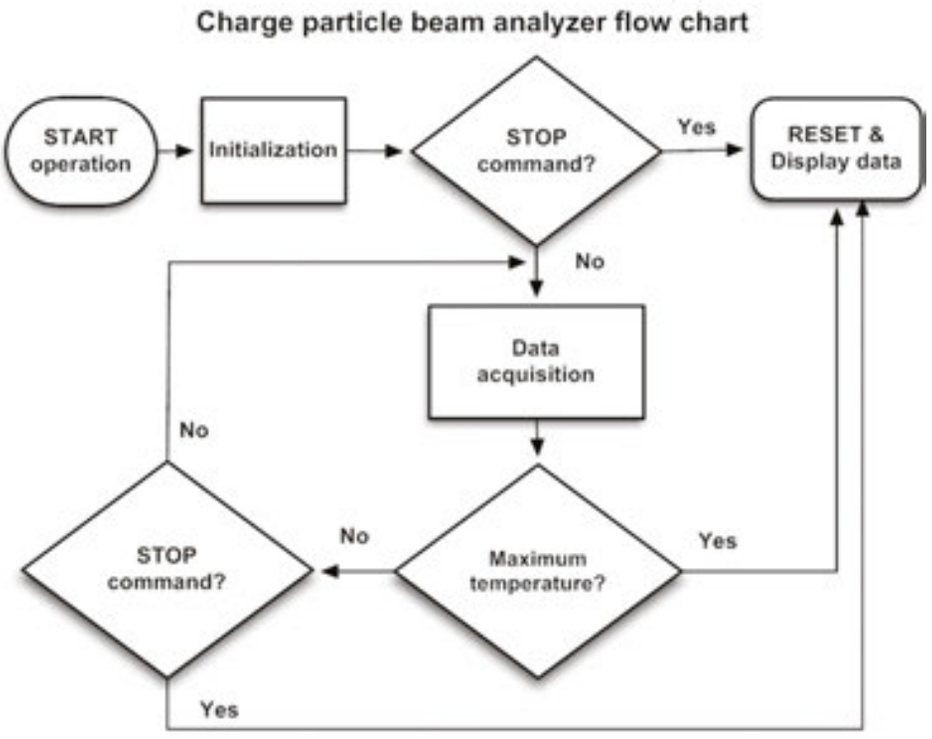

Figure 9. The flow chart of the electron beam analyzer.

During the "Initialization" step, the shutter is closed, the FBGs are cooled, and the functioning parameters set by the operator are introduced in the system. If a STOP command was issued by the operator the system stops and displays in 3D format the integrated energy to which each sensor was subjected, measured as Bragg wavelength shift in response to the local temperature increase. If no STOP command was given the system periodically acquires on the central wavelength shift for each sensor and checks if the maximum set temperature was reached by any of the FBGs. If this temperature was reached the system stops and displays the results as a 3D representation. If no such signal was received the software commands during the "Data acquisition" step the closing of the shutter and the cooling of the FBGs array. The periodicity of the cooling cycles, and the upper limit of the temperature to which any of the sensors can be subjected are set by the operator. The Bragg wavelength shift with the dose increase is given in **Figure 10**. In this case, during the irradiation pause, the grating's cooling

http://dx.doi.org/10.5772/62547

was obtained by convection in air and not by forced cooling. The proposed instrument can be used during the adjusting process of the charged particle accelerator or to check the stability in time of the output beam.

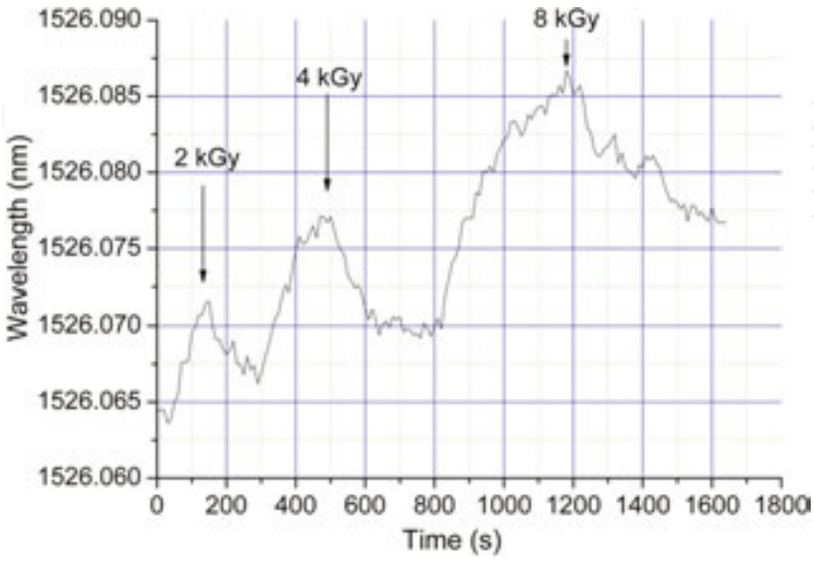

Figure 10. The change of the Bragg wavelength with the dose increase. Periodically, between two exposures the grating was cooled by natural convection [95].

A novelty in the field can be considered the investigation of FBGs performances written in polymer fibers under fast neutrons irradiation. In the paper it is suggested that neutrons produce a degradation of the fiber structure, which in turn causes a shift of the Bragg wavelength up to 14 pm. The wavelength change with neutron dose can be exploited in radiation dosimetry [96].

3.2. Long period gratings

Long period gratings (LPGs) were tested only under gamma ray exposure [90]. Most of the measurements were performed off-line [97–99], with some exceptions when the device behavior was monitored during the irradiation [100, 101]. The LPGs were obtained by different techniques: CO laser or UV engraving [99], electric arc-discharge (EAD) technique [101], CO_2 laser point-by-point writing [97], as chiral gratings [100], having a turnaround point (TAP) design produced by a CO_2 laser [98]. Various optical fibers were employed: N-doped and Ge-doped optical fibers [99], pure-silica-core/ F-doped silica cladding fibers [101], SMF-28™ [97], core doped with P, Ge, F, rare earth elements [100], photosensitive fibers (B/Ge co-doped) [98]. The irradiation conditions are modified from 5 kGy [97] up to 1.47 MGy [99]. Depending on the optical fiber type, the writing technique, the dose rate/total dose used, the reported results led to different conclusions: (i) no effect was observed on the LPG transmission spectrum for doses lower than 5 kGy [97], lower than 500 kGy [101] or as high as 1.47 MGy [99], (ii) a 10 nm shift of the transmission deep was noticed for doses of 100 kGy [100], (iii) very high shift of the dual resonance deep (35 nm) is present for a dose of 6 kGy [98]. This variety of investigations

outcomes suggest that, by an appropriate selection of the above mentioned parameters, LPGs can be produced either to be radiation hardened or with pronounced radiation sensitivity, appropriate to be used in radiation dosimetry. No change in the temperature sensitivity of LPGs upon irradiation was observed [101].

A new proposed approach in studying gamma irradiation effects on LGPs Includes several novelties [102, 103]:

- the use of an OFDR model LUNA OBR 4600, operating in the transmission mode or, for comparative purpose, of an optical fiber interrogator model sm125;
- LPGs on-line monitoring when the irradiation is on and off, which makes possible the observation of room temperature recovery;
- the comparative evaluation of the radiation induced LPG changes for grating produced in standard communication and specially designed radiation hardened optical fibers.

The use of the OFDR improved drastically the detection S/N as compared to classical reading with an optical spectrum analyzer. During the irradiation the sensors were encapsulated into ceramic radiation transparent cases to avoid any strain induced changes in the LPG spectrum, and in the mean time, the gratings were placed into a thermally insulated box. The temperature was permanently monitored both inside this box and in the irradiation chamber and temperature related corrections were applied to the LPG characteristics. Based on the referred papers, **Figure 11** illustrates comparatively the behaviour of gamma irradiation on the LPG developed into a standard communication optical fiber (LPGsc) and one written in a radiation hardened optical fiber (LPGrh). The wavelength deep of the two samples move in opposite directions, the wavelength of the grating produced in the standard communication fiber increases with the dose increase, while for the other one the wavelength decreases with the dose increase. Besides that, it can be noticed the magnitude of the two changes, LPGsc being by far more

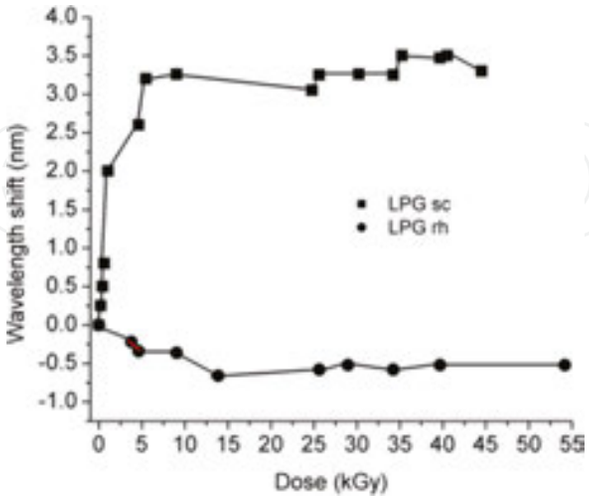

Figure 11. The change of the wavelength deep for two LPGs written in standard communication optical fibers LPGsc and in F-doped core optical fiber LPGrh.

sensitive. The fluctuations of the wavelength deep values during gamma exposure as well as the partial saturation trend are associated to the on-off operation of the irradiation facility. In this way, for the first time the recovery effect during the irradiation pauses was observed.

Because for the LPGrh the wavelength change is by far less significant than that in the case of LPGsc, it can be expected that the first one can be used in radiation environments as a sensor for temperature/humidity, while the second LPG can be employed within specific dose range as an optical fiber-based dosimeter.

4. Conclusions

The last four to five years brought additional data concerning radiation effects in optical fibers and optical fiber-based devices as new materials, technologies and possible applications in radiation environments emerged. In the frame of this chapter, the major trends were presented and some novel techniques and applications promoted recently were addressed, in relation to different types of irradiations (i.e. electron beam, synchrotron radiation). In this way, the data reviewed in previous publications are updated and the extensive possibilities offered by new materials and experimental setups in using radiation effects on optical fibers were demonstrated. By focusing such type of research on newly developed fibers (plastic, micro-structured, multi-core) and by using novel photonic devices based on optical fibers, new classes of equipment will emerge for terrestrial applications (dosimetry, medicine, remote and distributed monitoring) and for space missions.

Acknowledgements

The authors acknowledge the financial support of the Romanian Executive Agency for Higher Education, Research, Development and Innovation Funding (UEFISCDI), under grant 8/2012, project "Sensor Systems for Secure Operation of Critical Installations - SOCI" and of the Romanian Space Agency (ROSA) through the project "Evaluation of Components for Space Applications - ECSA", grant 67/ 2013.

Author details

Dan Sporea* and Adelina Sporea

*Address all correspondence to: dan.sporea@inflpr.ro

Photonics Investigations Laboratory, National Institute for Laser, Plasma and Radiation Physics, Magurele, Romania

References

[1] Sporea D, Agnello S, Gelardi FM. Irradiation effects in optical fibers. In: Pal B, editor. Frontiers in Guided Wave Optics and Optoelectronics. InTech; 2010. p. 46–66. DOI: 10.5772/303

[2] Sporea D, Sporea A, O'Keeffe S, McCarthy D, Lewis E, Optical fibers and optical fiber sensors used in radiation monitoring. In: Yasin M, Harun SW, Arof H, editors. Selected Topics on Optical Fiber Technology. InTech; 2012. p. 607-652. DOI: 10.5772/2429

[3] Berghmans F, Brichard B, Fernandez FA, Gusarov M, Van Uffelen M, Girard S. An introduction to radiation effects on optical components and fiber optic sensors. In: Bock WJ, Gannot I, Tanev S, editors. Optical Waveguide Sensing and Imaging, NATO Science for Peace and Security Series B: Physics and Biophysics. Springer; 2008. p. 127-165.

[4] Bourgade JL, Allouche A, Baggio J, Bayer C, Bonneau F, Chollet C, et al. New constraints for plasma diagnostics development due to the harsh environment of MJ class lasers. Rev. Sci. Instrum. 2004;75(10):4204-4212. DOI: http://dx.doi.org/10.1063/1.1789610

[5] Bourgade JL, Costley A.E, Reichle R, Hodgson ER, Hsing W, Glebov V, et al. Diagnostic components in harsh radiation environments: Possible overlap in R&D requirements of inertial confinement and magnetic fusion systems. Rev. Sci. Instrum. 2008;79:10F304. DOI: http://dx.doi.org/10.1063/1.2972024

[6] ITER. Available from: https://www.iter.org/mach [Accessed: January 29, 2016]

[7] Girard S, Baggio J, Leray J-L, Meunier J-P, Boukenter A, Ouerdane Y. Vulnerability analysis of optical fibers for Laser Megajoule Facility: Preliminary studies. IEEE Trans. Nucl. Sci. 2005;52(5):1497-1503. DOI: 10.1109/TNS.2005.855813

[8] Yamamoto S, Shikama T, Belyakov V, Farnum E, Hodgson E, Nishitani T,et al. Impact of irradiation effects on design solutions for ITER diagnostics. J. Nucl. Mater. 2000;283–287(1):60–69. DOI: 10.1016/S0022-3115(00)00157-4

[9] ELI-Nuclear Physics Working Groups. The White Book of ELI Nuclear Physics Bucharest-Magurele, Romania [Internet]. Available from: http://www.eli-np.ro/documents/ELI-NP-WhiteBook.pdf [Accessed: January 29, 2016]

[10] Delepine-Lesoille S, Pheron X, Bertrand J, Pilorget G, Hermand G, Farhoud R, et al. Industrial qualification process for optical fibers distributed strain and temperature sensing in nuclear waste repositories. J. Sensors. 2012;369375. DOI: 10.1155/2012/369375

[11] Wijnands TJ, De Jonge LK, Kuhnhenn J, Hoeffgen SK, Weinand U. Optical absorption in commercial single mode optical fibres for the LHC machine. Proceedings of the Topical Workshop on Electronics for Particle Physics [Internet], Prague, 3–7 September 2007, pp. 121-124. Available from: http://cds.cern.ch/record/1089249/files/p121.pdf [Accessed: January 29, 2016]

[12] Makovec A, Berruti G, Consales M, Giordano M, Petagna P, Buontempo S, et al. Radiation hard polyimide-coated FBG optical sensors for relative humidity monitoring in the CMS experiment at CERN. J. Instrum. 2014;9(03):C03040. DOI: 10.1088/1748-0221/9/03/C03040

[13] O'Keeffe S, McCarthy D, Woulfe P, Grattan MW, Hounsell AR, Sporea D, et al. A review of recent advances in optical fibre sensors for in-vivo dosimetry during radiotherapy. Br. J. Radiol. 2015;88:1050. DOI: http://dx.doi.org/10.1259/bjr.20140702

[14] Barth JL, Dyer CS, Stassinopoulos E.G. Space, atmospheric, and terrestrial radiation environments. IEEE Trans. Nucl. Sci. 2003;50(3):466-482. DOI: 10.1109/TNS.2003.813131

[15] Barth JL, LaBel KA, Poivey, C. Radiation assurance for the space environment. In: International Conference on Integrated Circuit Design and Technology ICICDT '04; Austin. 2004. p. 323-333. DOI: 10.1109/ICICDT.2004.1309976

[16] ECSS Secretariat. Space environment, ECSS-E-10-04A, ESA Publications Division [Internet], 2000. Available from: www.spacewx.com/Docs/ECSS-E-ST-10-04C_15Nov2008.pdf [Accessed: January 29, 2016]

[17] Schwank JR, Shaneyfelt MR, Dodd PE. Radiation hardness assurance testing of microelectronic devices and integrated circuits: Radiation environments, physical mechanisms, and foundations for hardness assurance. IEEE Trans. Nucl. Sci. 2013;60(3): 2074-2100. DOI: 10.1109/TNS.2013.2254722

[18] El-Kheshen AA. Glass as radiation sensor. In: Nenoi M, editors. Current Topics in Ionizing Radiation Research. InTech; 2012. p. 579-602. DOI: 10.5772/34612

[19] Farah K, Mejri A, Hosni F, Hamzaoui AH, Boizot B. Formation and decay of colour centres in a silicate glasses exposed to gamma radiation: Application to high-dose dosimetry. In: Nenoi M., editors. Current Topics in Ionizing Radiation Research. InTech; 2012. p. 603-624. DOI: 10.5772/32765

[20] Woody CL, Kierstead JA, Levy PW, Stoll S. Radiation damage in BaF2 crystals. IEEE Trans. Nucl. Sci. 1992;39:515-523. DOI: 10.1109/23.159658

[21] Li PJ, Xie YY, Zhao YL, Yin ZW. Radiation damage barium fluoride in large crystals [Internet], 1992. Available from: http://lss.fnal.gov/archive/other/ssc/ssc-gem-tn-92-000077.pdf [Accessed: January 29, 2016]

[22] El-Said AS, Cranney M, Ishikawa N, Iwase A, Neumann R, Schwartz K, et al. Study of heavy-ion induced modifications in BaF2 and LaF3 single crystals. Nucl. Instrum. Methods B. 2004;218:492–497. DOI: 10.1016/j.nimb.2003.12.057

[23] Izerrouken M, Meftah A, Nekka M. Color centers in neutron-irradiated Y3Al5O12, CAF2 and LiF single crystals. J. Lumin. 2007;127:696–702. DOI: 10.1016/j.jlumin. 2007.04.005

[24] Fernández-Rodríguez M, Alvarado CG, Núñez A, Álvarez-Herrero A. Analysis of optical properties behaviour of Clearceram, fused silica and CaF2 glasses exposed to

simulated space conditions. In: Proceedings of the International Conference on Space Optics (ICSO 2010), 4–8 October 2010. Available from: http://www.congrexprojects.com/custom/ icso/Papers/Session%2011a/FCXNL-10A02-2018721-1-FERNANDEZ-RODRIGUEZ_ICSO_ PAPER.pdf

[25] Brovetto B, Maxia V, Salis M. On the radioluminescent emission of BaF2. Il Nuovo Cimento D. 1996;18(9):1107-1110. DOI: 10.1007/BF02457676

[26] Dafinei I, Fasoli M, Ferroni F, Mihokova E, Orio F, Pirro S, et al. Low temperature scintillation in ZnSe crystals. IEEE Trans. Nucl.Sci. 2010;57(3):1470-1474. DOI: 10.1109/TNS.2009.2035914

[27] Yanagida T, Fujimoto Y, Koshimizu M, Fukuda K. Scintillation properties of CdF2 crystal. J. Lumin. 2015;157:293–296. DOI: http://dx.doi.org/10.1016/j.jlumin.2014.09.013

[28] Kristianpoller N, Rehavi A, Shmilevich A, Weiss D, Chen R.Radiation effects in pure and doped Al2O3 crystals. Nucl. Instrum. Meth B. 1998;141:343-346. DOI: 10.1016/S0168-583X(98)00096-2

[29] Plaksin OA, Stepanov VA, Demenkov PV, Stepanov PA, Skuratov VA, Kishimoto N. Radioluminescence of alumina during proton and heavy ion irradiation. Nucl. Instrum. Methods B. 2003;206:1083–1087. DOI: 10.1016/S0168-583X(03)00915-7

[30] Islamov AKh, Ibragimova EM, Nuritdinov I. Radiation-optical characteristics of quartz glass and sapphire. J. Nucl. Mater. 2007;362:222–226. DOI: 10.1016/j.jnucmat.2007.01.047

[31] Izerrouken M, Benyahia T. Absorption and photoluminescence study of Al2O3 single crystal irradiated with fast neutrons. Nucl. Instrum. Methods B. 2010;268:2987-2990. DOI: 10.1016/j.nimb.2010.05.024

[32] Zhang MF, Zhang HL, Han JC, Guo HX, Xu CH, Ying GB. Effects of neutron irradiation and subsequent annealing on the optical characteristics of sapphire. Effects of neutron irradiation and subsequent annealing on the optical characteristics of sapphire. Physica B. 2011;406:494–497. DOI: 10.1016/j.physb.2010.11.021

[33] Faist J, Capasso F, Sivco DL, Sirtori C, Hutchinson AL, Cho AY. Quantum cascade laser. Science. 1994;264(5158):553-556. DOI: 10.1126/science.264.5158.553

[34] Wilson CF, Chassefière E, Hinglais E, Baines KH, Balint TS, Berthelier J-J, et al. The 2010 European Venus Explorer (EVE) mission proposal. Exp. Astron. 2012;33(2):305-335. DOI: 10.1007/s10686-011-9259-9

[35] Forouhar S, Borgentun C, Frez C, Briggs R, Bagheri M, Webster CR, et al. Mid-IR semiconductor lasers for space. In: Mid-Infrared Optoelectronics: Materials and Devices (MIOMD-XII); 5–9 October 2014; Montpellier, France.

[36] Mihai L, Sporea D, Sporea A. Vâţă I. Testing of ZnSe, CaF2, BaF2, and sapphire windows under alpha particles irradiation. In: 3rd International Conference and Exhibition on Lasers, Optics and Photonics; 1–3 September 2015; Valencia, Spain.

[37] Mihai L, Sporea D, Sporea A, Ighigeanu D, Neguţ D. Optical and THz evaluation of components for gas sensing spectroscopy in hazardous environments. In: NATO ARW on THz Diagnostics of CBRN effects and Detection of Explosives & CBRN; 3–6 November 2015; Izmir, Turkey.

[38] Mihai L, Sporea D, Sporea A, Craciun G, Manaila E. Electron beam irradiation of materials and components to be used in mid-IR spectroscopy. In: Photonics Europe 2016; 3–7 April, 2016; Brussels, Belgium. paper EPE117-144.

[39] Girard S, Kuhnhenn J, Gusarov A, Brichard B, Van Uffelen M, Ouerdane Y, et al. Radiation effects on silica-based optical fibers: Recent advances and future challenges. IEEE Trans. Nucl. Sci. 2013;60(3):2015-2036. DOI: 10.1109/TNS.2012.2235464

[40] Griscom DL. A minireview of the natures of radiation-induced point defects in pure and doped silica glasses and their visible/near-IR absorption bands, with emphasis on self-trapped holes and how they can be controlled. Phys Res Int. 2013;ID 379041. DOI: http://dx.doi.org/10.1155/2013/379041

[41] Paul MC, Sen R, Bhadra SK, Pal M, Giri PP, Dasgupta K, et al. Gamma ray radiation induced absorption in Ti doped single mode optical fibres at low dose levels. Opt. Mater. 2007;29:738–745. DOI: 10.1016/j.optmat.2005.12.004

[42] Paul MC, Sen R, Bhadra SK, Dasgupta K. Radiation response behaviour of Al codoped germano-silicate SM fiber at high radiation dose. Opt. Commun.. 2009;282:872–878. DOI: 10.1016/j.optcom.2008.11.052

[43] Paul MC, Bohra D, Dhar A, Sen R, Bhatnagar PK, Dasgupta K. Radiation response behavior of high phosphorous doped step-index multimode optical fibers under low dose gamma irradiation. J. Non-Cryst. Solids. 2009;355:1496-1507. DOI: 10.1016/j.jnoncrysol.2009.05.017

[44] Ghosh S, Das S, Paul MC, Dasgupta K, Bohra D, Chaudhary HS,et al. Evaluation of the performance of high phosphorous with germanium codoped multimode optical fiber for use as a radiation sensor at low dose rates. Appl. Opt. 2011;50(25):E80-E85. DOI: 10.1364/AO.50.000E80

[45] Jin J, Liu J, Xu J. Effect of spectral dependencies of radiation-induced attenuation in polarization maintaining fibers on interferometric fiber optic gyroscope at near-infrared wavelengths. Optik. 2013;124:5679-5682. DOI: http://dx.doi.org/10.1016/j.ijleo.2013.04. 057

[46] Kim Y, Ju S, Jeong S, Kim JY, Lee NH, Jung HK, et al. Gamma-ray irradiation-induced optical attenuation in Co/Fe co-doped alumino-silicate optical fiber for dosimeter

application. J. Lightwave Technol. . 2014;32(22):3791-3797. DOI: 10.1109/JLT.2014.2357798

[47] Kir'yanov AV, Ghosh S, Paul MC, Barmenkov YO, Aboites V, Kozlova NS. Ce-doped and Ce/Au-codoped alumino-phosphosilicate fibers: Spectral attenuation trends at high-energy electron irradiation and posterior low-power optical bleaching. Opt. Mater. Express. 2014;4(3):434-448. DOI: 10.1364/OME.4.000434

[48] Girard S, Marcandella C, Morana A, Perisse J, Di Francesca D, Paillet P, et al. Combined high dose and temperature radiation effects on multimode silica-based optical fibers. IEEE Trans. Nucl. Sci. 2013;6(6):4305-4313. DOI: 10.1109/TNS.2013.2281832

[49] Di Francesca D, Boukenter A, Agnello S, Girard S Alessi A, Paillet P, et al. X-ray irradiation effects on fluorine-doped germanosilicate optical fibers. Opt. Mater. Express. 2014;4(8):1683-1695. DOI: 10.1364/OME.4.001683

[50] Sporea D, Sporea A, Oproiu C. Effects of hydrogen loading on optical attenuation of gamma-irradiated UV fibers. J. Nucl. Mater. 2012;423(1-3):142-148. DOI: 10.1016/j.jnucmat.2012.01.023

[51] Sporea D, Mihai L, Sporea A, Lixandru A, Bräuer-Krisch E. Investigation of UV optical fibers under synchrotron irradiation. Opt. Express. 2014;22(25):31473-31485. DOI: 10.1364/OE.22.031473

[52] Girard S, Ouerdane Y, Marcandella C, Boukenter A, Quenard S, Authier N. Feasibility of radiation dosimetry with phosphorus-doped optical fibers in the ultraviolet and visible domain. J. Non-Cryst. Solids. 2011;357:1871-1874. DOI: 10.1016/j.jnoncrysol.2010.11.113

[53] Tomashuk AL, Grekov MV, Vasiliev SA, Svetukhin VV. Fiber-optic dosimeter based on radiation-induced attenuation in P-doped fiber: suppression of post-irradiation fading by using two working wavelengths in visible range. Opt Express. 2014;22(14):16779-16783. DOI: 10.1364/OE.22.016778

[54] Stajanca P, Sporea D, Mihai L, Negut D, Schukar M, Krebber K. Gamma radiation induced effects on perfluorinated polymer optical fibers for sensing applications. In: Bunge C-A, Kruglov R, editors. Perfluorinated Polymer Optical Fibers for Sensing Applications. BoD - Books on Demand: Norderstedt; 2015. ISBN 978-3-7392-1499-3.

[55] Mihai L, Sporea D, Negut D, Stajanca P, Krebber K. On-line monitoring of gamma irradiated perfluorinated polymer optical fiber. In: Photonics Europe 2016; 3–7 April, 2016; paper EPE104-58.

[56] Sporea D, Sporea A. Radiation effects in sapphire optical fibers. Physica Status Solidi (c). 2007;4(3):1356–1359. DOI: 10.1002/pssc.200673709

[57] Petrie ChM, Windl W, Blue ThE. In-situ reactor radiation-induced attenuation in sapphire optical fibers. J. Am. Ceram. Soc. 2014;97:3883-3889. DOI: 10.1111/jace.13211

[58] Petrie ChM, Wilson B, Blue ThE. In situ gamma radiation-induced attenuation in sapphire optical fibers heated to 1000°C. J. Am. Ceram. Soc. 2014;97:3150-3156. DOI: 10.1111/jace.13089

[59] Phéron X, Girard S, Boukenter A, Brichard B, Delepine-Lesoille S, Bertrand J,et al. High γ-ray dose radiation effects on the performances of Brillouin scattering based optical fiber sensors. Opt. Express. 2012;20(24):26978-26985. DOI: 10.1364/OE.20.026978

[60] Faustov A, Gusarov A, Wuilpart M, Fotiadi AA, Liokumovich LB, Kotov OI, et al. Distributed optical fibre temperature measurements in a low dose rate radiation environment based on Rayleigh backscattering. In: Berghmans F, Mignani AG, De Moor P, editors. Proceedings of Optical Sensing and Detection II; SPIE 8439: 84390C; 2012. DOI: 10.1117/12.922082

[61] Toccafondo I, Brugger M, Di Pasquale F, Guillermain E, Kuhnhenn J. First steps towards a distributed optical fiber radiation sensing system. International Conference on Space Optics, Tenerife, Canary Islands, Spain [Internet], 7–10 October 2014. Available from: http://congrexprojects.com/Custom/ICSO/2014/Papers/5.%20Posters/Poster%20Session%202/2.10.66978_Toccafondo.pdf [Accessed: January 29, 2016]

[62] Faustov AV, Gusarova A, Wuilpart M, Fotiadi A, Liokumovichc LB, Zolotovskiyf IO, at al. Remote distributed optical fibre dose measuring of high gamma-irradiation with highly sensitive Al- and P-doped fibres. In: Baldini F, Homola J, Lieberman RA, editors. Proceedings of Optical Sensors 2013; SIPE 8774:877404; 2013. DOI: 10.1117/12.2017331

[63] Brichard B, Fernandez, AF, Ooms H, Berghmans F. Gamma dose rate effect in erbium-doped fibers for space gyroscopes. In: Proceedings of the 16th International Conference on Optical Fiber Sensors OFS16, Nara, 13–17 October 2003, pp. 336-339. Available from: https://www.researchgate.net/profile/Francis_Berghmans/publication/228759091_Gamma_Dose_Rate_Effect_in_Erbium-Doped_Fibers_for_Space_Gyroscopes/links/09e4150b625689e300000000.pdf [Accessed: January 29, 2016]

[64] Brichard B, Fernandez AF, Ooms H, van Uffelen M, Berghmans F. Study of the radiation-induced optical sensitivity in erbium and aluminium doped fibres. In: Proceedings of the 7th European Conference on Radiation and Its Effects on Components and Systems RADECS2003, Noordwijk, 15–19 September 2003, pp. 35-38. Available from: http://citeseerx.ist.psu.edu/viewdoc/download?doi=10.1.1.59.2175&rep=rep1&type=pdf [Accessed: January 29, 2016]

[65] Lezius M, Predehl K, Stower W, Turler A, Greiter M, Hoeschen C, et al. Radiation induced absorption in rare earth doped optical fibers. IEEE Trans. Nucl. Sci. 2012;59(2):425-433. DOI: 10.1109/TNS.2011.2178862

[66] Girard S, Ouerdane Y, Tortech B, Marcandella C, Robin T, Cadier B, et al. Radiation effects on Ytterbium- and Ytterbium/Erbium-doped double-clad optical fibers. IEEE Trans. Nucl. Sci. 2009;56(6):3293-3399. DOI: 10.1109/TNS.2009.2033999

[67] Rose TS, Gunn D, Valley GC. Gamma and proton radiation effects in Erbium-doped fiber amplifiers: active and passive measurements. J. Lightwave Technol. 2001;19(12): 1918-1923. DOI: 10.1109/50.971685

[68] Chang SH, Liu R-Y, Lin C-E, Chou F-I, Tai C-Y, Chen CC. Photo-annealing effect of gamma-irradiated erbium-doped fibre by femtosecond pulsed laser. J. Phys. D: Appl. Phys. 2013;46:495113-495119. DOI: 10.1088/0022-3727/46/49/495113

[69] Peng T-S, Huang Y-W, Wang LA, Liu R-Y, Chou F-I. Photo-annealing effects for Erbium doped fiber sources after gamma irradiation tests by using 532 nm and 976 nm lasers. In: Jones J, Culshaw B, Ecke W, López-Higuera JM, Willsch R, editors. Proceedings of the 20th International Conference on Optical Fibre Sensors; SPIE 7503: 750375; 2009. DOI: 10.1117/12.835304

[70] Ma J, Li M, Tan L-Y, Zhou Y-P, Yu S-Y, Che C. Space radiation effect on EDFA for inter-satellite optical communication. Optik - Int. J. Light Electron Opt. 2010;121(6):535-538. DOI: 10.1016/j.ijleo.2008.09.009

[71] Singleton BJ. Radiation Effects on Ytterbium-doped Optical Fibers. No. AFIT-ENP-DS-14-J-15, Air Force Institute of Technology Wright-Patterson AFB OH Graduate School of Engineering and Management [Internet], 2014. Available from: http://www.dtic.mil/cgi-bin/GetTRDoc?Location=U2&doc=GetTRDoc.pdf&AD=ADA602890 [Accessed: January 29, 2016]

[72] Fox BP. [thesis]. Investigation of ionizing-radiation-induced photodarkening in rare-earth-doped optical fiber amplifier materials, The University of Arizona; 2013.

[73] Mady F, Benabdesselam M, Mebrouk Y, Dussardier B. Radiation effects in ytterbium-doped silica optical fibers: traps and color centers related to the radiation-induced optical losses. In: Proceedings of RADECS 2010, Paper LN2; 2010. Available from: https://hal.archives-ouvertes.fr/hal-00559422/file/Paper_LN2.pdf [Accessed: January 29, 2016]

[74] Zotov KV, Likhachev ME, Tomashuk AL, Kosolapov AF, Bubnov MM, Yashkov MV, et al. Radiation resistant Er-doped fibers: optimization of pump wavelength. IEEE Photonics Technol. Lett. 2008;20(17):1476–1478. DOI: 10.1109/LPT.2008.927909

[75] Zotov KV, Likhachev ME, Tomashuk AL, Bubnov MM, Yashkov MV, Guryanov AN, et al. Radiation-resistant erbium-doped fiber for spacecraft applications. IEEE Trans. Nucl. Sci. 2008;55(4):2213-2215. DOI: 10.1109/TNS.2008.2001834

[76] Thomas J, Myara M, Troussellier L, Burov E, Pastouret A, Boivin D, et al. Radiation-resistant erbium-doped-nanoparticles optical fiber for space applications. Opt. Express. 2012;20(3):2435-2444. DOI: 10.1364/OE.20.002435

[77] Girard S, Mescia L, Vivona M, Laurent A, Ouerdane Y, Marcandella C, et al. Design of radiation-hardened rare-earth doped amplifiers through a coupled experiment/

simulation approach. J. Lightwave Technol. 2013;31(8):1247-1254. DOI: 10.1109/JLT.2013.2245304

[78] Hamdalla, TA, Nafee SS. Radiation effects on the gain of thulium doped fiber amplifier: Experiment and modeling. Opt. Laser Technol. 2014;55:46-49. DOI: 10.1016/j.optlastec.2013.06.024

[79] Luo Y, Wen J, Zhang J, Canning J, Peng G-D. Bismuth and erbium codoped optical fiber with ultrabroadband luminescence across O-, E-, S-, C-, and L-bands. Opt. Lett. 2012;37(16):3447-3449. DOI: 10.1364/OL.37.003447

[80] Yan B, Luo Y, Sporea D, Mihai L, Neguţ D, Sang X, et al. Gamma radiation-induced formation of bismuth related active centre in Bi/Er/Yb co-doped fibre. In: Asia Communications and Photonics Conference (ACP); 19–23 November 2015; Hong Kong.

[81] Wen J, Liu W, Dong Y, Luo Y, Peng G-D, Chen N, et al. Radiation-induced photoluminescence enhancement of Bi/Al-codoped silica optical fibers via atomic layer deposition. Opt. Express. 2015;23(22):29004-29013. DOI: 10.1364/OE.23.029004

[82] Sporea D, Mihai L, Negut D, Luo Y, Yan B, Ding M, et al. Effects of gamma rays on rare Bi/Er co-doped optical fibers. In: ROMOPTO2015 Conference; 1–4 September 2015; Bucharest, Romania.

[83] Butov OV, Golant KM, Shevtsov IA, Fedorov AN. Fiber Bragg gratings in the radiation environment: Change under the influence of radiolytic hydrogen. J. Appl. Phys. 2015;118:074502. DOI: 10.1063/1.4928966

[84] Fernandez AF, Brichard B, Berghmans F, Decréton M. Dose-rate dependencies in gamma-irradiated fiber Bragg grating filters. IEEE Trans. Nucl.Sci. 2002;49(6): 2874-2878. DOI: 10.1109/TNS.2002.805985

[85] Fielder RS, Klemer D, Stinson-Bagby KL. High neutron fluence survivability testing of advanced fiber Bragg grating sensors. In: AIP Conference Proceedings on Thermophysics in Microgravity; Commercial/Civil Next Generation Space Transportation; 21st Symposium Space Nuclear Power & Propulsion; Human Space Explorer; Space Colonization; New Frontiers & Future Concepts; 2004, Vol. 699, pp. 650-657. DOI: http://dx.doi.org/10.1063/1.1649627

[86] Fernandez AF, Brichard B, Berghmans F, Rabii H, Fokine M, Popov M. Chemical composition fiber gratings in a high mixed gamma neutron radiation field. IEEE Trans. Nucl. Sci. 2006;53(3):1607-1613. DOI: 10.1109/TNS.2005.863273

[87] Gusarov A, Fernandez AF, Vasiliev S, Medvedkov O, Blondel M, Berghmans F. Effect of gamma–neutron nuclear reactor radiation on the properties of Bragg gratings written in photosensitive Ge-doped optical fiber. Nucl. Instrum. Methods B. 2002;187(1):79-86. DOI: 10.1016/S0168-583X(01)00829-1

[88] Perry M, Niewczas P, Johnston M. Effects of neutron-gamma radiation on fiber Bragg grating sensors: a review. IEEE Sensors. 2012;12(11):3248-3257. DOI: 10.1109/JSEN.2012.2214030

[89] Curras E, Virto AL, Moya D, Vila I, Carrión JG, Frövel M, Palomo FR. Influence of the fiber coating type on the strain response of proton-irradiated fiber Bragg gratings. IEEE Trans. Nucl.Sci. 2012;59(4):937-942. DOI: 10.1109/TNS.2012.2206049

[90] Gusarov A, Hoeffgen SK. Radiation effects on fiber gratings. IEEE Trans. Nucl. Sci. 2013;60(3):2037-2053. DOI: 10.1109/TNS.2013.2252366

[91] Maier RRJ, MacPherson WN, Barton JS, Jones JDC, McCulloch S, Fernandez AF, et al. Fibre Bragg gratings of type I in SMF-28 and B/Ge fibre and type IIA B/Ge fibre under gamma radiation up to 0.54 MGy. In: Proceedings of SPIE 17th International Conference on Optical Fibre Sensors, 2005, Vol. 5855, pp. 511-514. DOI: 10.1117/12.624037

[92] Faustov A, Saffari P, Koutsides C, Gusarov A, Wuilpart M, Mégret P, et al. Highly radiation sensitive type IA FBGs for future dosimetry applications. IEEE Trans. Nucl. Sci. 2012;59(4):1180-1185. DOI: 10.1109/TNS.2012.2202247

[93] Krebber K, Henschel H, Weinand U. Fibre Bragg gratings as high dose radiation sensors? Meas. Sci. Technol. 2006;17:1095-1102. DOI: 10.1088/0957-0233/17/5/S26

[94] de Villiers GJ, Treurnicht J, Dobson RT. In-core high temperature measurement using fiber-Bragg gratings for nuclear reactors. Appl. Therm. Eng. 2012;38:143-150. DOI: 10.1016/j.applthermaleng.2012.01.024

[95] Sporea D, Stancalie A, Becherescu N, Becker M, Rothhardt M. An electron beam profile instrument based on FBGs. Sensors 2014. 2014;14(9):15786-15801. DOI: 10.3390/s140915786

[96] Hamdalla TA, Nafee SS. Bragg wavelength shift for irradiated polymer fiber Bragg grating. Opt. Laser Technol. 2015;74:167–172. DOI: 10.1016/j.optlastec.2015.06.008

[97] Chaubey S, Joshi P, Kumar M, Arya R, Nath AK, Kher S. Design and development of long-period grating sensors for temperature monitoring. Sādhanā. 32(5):513-519.

[98] Kher S, Chaubey S, Kashyap R, Oak SM. Turnaround-Point Long period fiber gratings (TAP-LPGS) as high radiation dose sensors. IEEE Photonics Technol. Lett. 2012;24(9):742-744. DOI: 10.1109/LPT.2012.2187637

[99] Vasiliev SA, Dianov EM, Golant KM, Medvedkov OI, Tomashuk AL, Karpov VI,et al. Performance of Bragg and long-period gratings written in N- and Ge-doped silica fibers under y-radiation. IEEE Trans. Nucl. Sci. 1998;45(3):1580-1583. DOI: 10.1109/23.685243

[100] Henschel H, Hoeffgen SK, Kuhnhenn J, Weinand U. High radiation sensitivity of chiral long period gratings. IEEE Trans. Nucl. Sci. 2010;57(5):2915-2922. DOI: 10.1109/TNS.2010.2059043

[101] Rego G, Fernandez AF, Gusarov G, Brichard B, Berghmans F, Santos JL. Effect of ionizing radiation on the properties of arc-induced long-period fiber gratings. App. Opt. 2005;44(29):6258-6263. DOI: 10.1364/AO.44.006258

[102] Sporea D, Stancălie A, Negut D, Pilorget G, Delepine-Lesoille S, Lablonde L. On-line tests of an optical fiber long-period grating subjected to gamma irradiation. IEEE Photonics J. 2014;6(6):1-9. DOI: 10.1109/JPHOT.2014.2337877

[103] Sporea D, Stăncalie A, Neguţ D, Pilorget G, Delepine-Lesoilled S, Lablonde L. Comparative study of long period and fiber Bragg gratings under gamma irradiation. Sensor Actuator A-Phys. 2015;233:295-301. DOI: http://dx.doi.org/10.1016/j.sna.2015.07.007

IntechOpen